

Modeling Urban Atmospheric Lead Dispersion from a Mining Tailings Basin in Bahia, Brazil

Modelagem de Dispersão Atmosférica Urbana de Chumbo de uma Bacia de Rejeitos de Mineração na Bahia, Brasil

Nelize Lima dos Santos , Harald Klammler  & Luiz Rogério Bastos Leal 

Universidade Federal da Bahia, Instituto de Geociências, Programa de Pós-Graduação em Geologia, Salvador, BA, Brasil

E-mails: nelize@ufba.br; haki@ufl.edu; lrogerio@ufba.br

Corresponding author: Nelize Lima dos Santos; nelize@ufba.br

Abstract

After the exhaustion of the lead mine in Boquira, Bahia in the 1990s, mining support structures and the tailings basin were abandoned, resulting in one of the largest environmental liabilities from mining in the state. Detailed studies on environmental damages are inexistent and this article aimed to analyze lead contamination in the urban area of the municipality, based on atmospheric dispersion modeling. For this purpose, a model was elaborated and implemented in Matlab R2014a considering houses, streets and air as three coexisting spatial domains. The model uses wind speed and direction as input data and results were calibrated (RMSE = 0.64 on decadal logarithmic scale) against existing measurements taken in 2014 of lead concentrations in street sediments and house dust within the urban area. Results suggested that particulate resuspension from streets and accumulation in houses may explain observed concentration patterns, and that the amount of suspended lead in the air is small compared to that in streets and houses. Additional simulations carried out for a hypothetical future remediation scenario showed that after 200 days the concentrations in the air and in the streets decreased considerably, while they stopped accumulating in houses. Hence, the model may be a potentially useful tool to assist in the evaluation and management of this and other urban areas affected by contamination through atmospheric dispersion of particulates. Consistent with our model formulation, we recommend mass per area for lead concentrations in streets and houses as more meaningful units for exposure risk/intensity than ppm (mass per mass) of street sediment or house dust.

Keywords: Abandoned mining; Atmospheric transport; Numerical model

Resumo

Após a exaustão da mina de chumbo em Boquira, Bahia, nos anos 90, as estruturas de apoio da mineração e a bacia de rejeito foram abandonadas, resultando num dos maiores passivos ambientais provenientes da mineração no estado. Não existem estudos detalhados sobre danos ambientais e este artigo teve como objetivo analisar a contaminação de chumbo na zona urbana do município, a partir da modelagem de dispersão atmosférica. Para isso, foi elaborado um modelo com três domínios (casas, ruas e ar) no *software* Matlab R2014a, tendo como dados de entrada as informações referentes às condições meteorológicas da região, especificamente, direção e velocidade dos ventos. Utilizamos para calibração (RMSE = 0,64 em logaritmos decimais) as análises químicas de contaminação de chumbo obtidas em 2014 em sedimentos de rua e poeiras de casas distribuídas ao longo da zona urbana. Os resultados sugeriram que a ressuspensão de partículas em ruas e a acumulação em casas podem explicar padrões observados de concentrações, e que a quantidade de chumbo suspenso no ar é pequena comparado com ruas e casas. Simulações adicionais para um cenário futuro hipotético de remediação da bacia de rejeitos demonstrou que após 200 dias as concentrações no ar e nas ruas diminuiriam consideravelmente e nas casas pararia de acumular. Desta forma, o modelo demonstrou potencialidade para auxiliar na avaliação e gestão desta e outras áreas contaminadas através da dispersão atmosférica de partículas. Coerente com nosso modelo, recomendamos o uso de massa por área para concentrações de chumbo em ruas e casas como unidades mais apropriadas para risco/intensidade e exposição que ppm (massa por massa) de sedimentos ou poeira.

Palavras-chave: Mineração abandonada; Transporte atmosférico; Modelo numérico

1 Introduction

Mining activities are a corner stone of global economy and although mining creates economic growth, it also causes socio-economic disequilibrium and environmental pollution. The environmental legislation in Brazil recognizes mineral extraction as an activity of public utility and social interest. Municipalities are regulated by resolution CONAMA 491/2018 about air quality and CONAMA 420/2009 defining quality standards for soil and establishing guidelines for environmental management of areas contaminated by anthropic activities. However, the inefficient handling of potentially adverse impacts has resulted in environmental deterioration and, consequently, prejudice to human health.

Lead occurs naturally in the environment and, although it is widely used in industrial activities, exposure causes harmful reactions in biological organisms, thus posing a serious risk to ecosystems and human health (Chen et al. 2022; Christou et al. 2022; Huang et al. 2020; Teixeira et al. 2020). The World Health Organization (WHO 2017) states that there is no safe level of lead exposure, which is why it is fundamental to understand the sources and various transport paths of this metal to avoid health damages. The most important lead exposure mechanisms are ingestion and inhalation. Most cases of oral intoxication result from repeated ingestion of small lead quantities in contaminated dust or soil. The inhalation of lead in the form of smoke or particulates is the principal occupational exposure path (WHO 2021).

The semi-arid region of Bahia was once the largest producer of lead in Brazil. From 1956 to 1992, the Boquira mine produced more than six million tons of ore (Carvalho et al. 1997), whose tailings were deposited in a basin of approximately 33600 m² in area and 894000 m³ in volume (Santos, Anjos & Klammler 2020). Studies indicated instability of the tailings basin with susceptibility to wind erosion and a series of water erosion channels. These processes transport lead contaminated material to the urban area of the municipality and to a tributary of the Paramirim River, the largest river in the region. The climatic adversities of the semi-arid region are characterized by low and irregular rainfall events as well as long cyclical droughts. Moreover, concentrations of heavy metals found in groundwater, springs and cisterns of the municipality are low (Gomes, Anjos & Daltro 2020). These facts contributed to the formulation of the hypothesis that wind erosion and transport would be the main processes causing the dispersion of lead (and other contaminants) originating from the tailings basin across the urban area of Boquira.

A global evaluation of pollution exposure also indicated that air pollution represents the largest environmental risk to public health at present (WHO 2016). As a consequence, health related estimates of atmospheric pollution exposure and impacts are fundamental for the formulation of policies supporting public health preservation. Atmospheric dispersion models are useful tools for predicting air quality and identifying areas and/or time periods of pollutant concentrations above established legal limits (Borges, Teixeira & Ribeiro 2021; Costa & Costa 2021). Such models consider transport processes including the mechanisms of suspension, advection, dispersion, deposition, resuspension and/or accumulation (Khan & Hassan 2021). Contaminants can be removed from the atmosphere by dry deposition processes through the action of gravity, and also by wet deposition consisting of the absorption of pollutants by raindrops and consequent removal by precipitation to the soil.

The mathematical modeling of atmospheric transport is based on the numerical solution of the mass conservation equation of a chemical species. These models can be used to identify and study standard scenarios as well as for site assessment and simulation of predictions, thus supporting solutions to problems of air pollution. The atmospheric dispersion of suspended particulates is related to local turbulence and deposition, including downward movement due to precipitation and sedimentation (Khan & Hassan 2021; Leelossy et al. 2018). According to Seinfeld and Pandis (2006), the deposition process consists of three distinct steps being (1) aerodynamic transport to a very thin layer of stagnant air adjacent to the surface, (2) Brownian transport in this very thin layer, and (3) adherence at the surface.

There is a variety of existing atmospheric transport simulation models, which can be largely categorized into either Eulerian (based on concentrations as a function of location and time) or Lagrangian (based on clouds of moving particles). Such models have been applied for investigating health impacts of air pollution (Andreão et al. 2020), long-range transport (Duarte et al. 2021) and scenarios for the reduction of contaminant emissions (Teixeira et al. 2020; Zhang et al. 2021). For more comprehensive reviews see Giovannini et al. (2020), Khan and Hassan (2021), or Leelossy et al. (2018).

However, despite the elevated risks and damages associated with lead contamination in general, and the reported contamination due to the tailings basin in Boquira, we are not aware of (1) an existing atmospheric dispersion model, which implicitly considers contaminant concentrations in the atmosphere, streets and houses as

coupled spatio-temporal variables, and (2) a mathematical modeling effort of the atmospheric lead dispersion between the Boquira tailings basin and the adjacent urban area. In the present study, we develop and implement such a model in a Eulerian framework to demonstrate its calibration and performance for atmospheric lead contamination in Boquira. Results match the distinct contrast in observed concentrations between streets and houses and the model is applied to the hypothetical future scenario of source remediation (e.g., complete basin coverage). This demonstrates its usefulness for the evaluation of areas contaminated by aerial particulate transport as well as for environmental management and planning more generally.

2 Methodology

2.1 Study Area and Data

The study area is located in the center of the state of Bahia, Brazil (Figure 1A). In geotectonic terms, it is inserted in the domain of the São Francisco craton and divided between the Paramirim deformation corridor and the Espinhaço Setentrional (Alkimim, Brito Neves & Alves 1993). The geomorphological contrast between these compartments is clear due to the steep and dissected slopes of the Serra do Espinhaço, whose orientation is NW-SE and reaches altitudes above 1100 m.

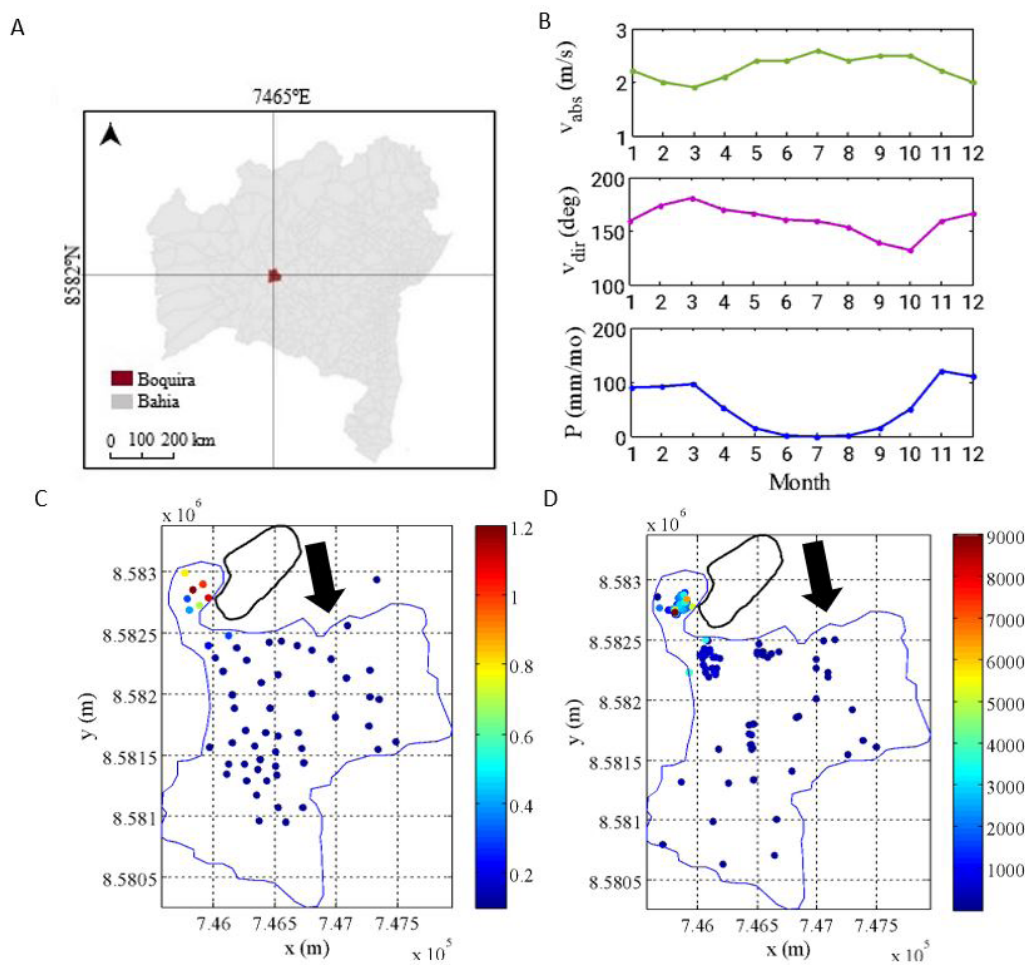


Figure 1 Characterization of the area: A. Location of Boquira municipality within the state of Bahia, Brazil; B. Monthly averages of wind speed v_{abs} , wind direction v_{dir} , and rainfall intensity P ; C. Measured lead concentrations in street sediments; D. Measured lead concentrations in house dust. The color bars in C. and D. are in ppm and the coordinates are UTM with datum SIRGAS 2000, showing the limits of the urban area (blue line) and the tailings basin (black line). Wind direction represents the simple arithmetic (i.e., time weighted) average of hourly measurements in degrees clockwise from North (see black arrow in C. and D. for overall mean direction and Santos et al. 2020, for graphics of wind roses).

In contrast, the Paramirim Valley corresponds to a large plain with altitudes ranging between 400 and 700 m (Garcia 2011). Among other lithotypes, this geotectonic domain comprises rocks of the Boquira Complex, which constitutes a Greenstone belt sequence, embedded in Pb-Zn mineralization (Garcia 2011).

The natural context of the rocks of the municipality of Boquira influences the chemical composition of water resources (Gomes, Anjos & Daltro 2020). However, the highest concentrations of metals such as lead and zinc were located in the waters of the underground mine galleries, but high metal contents were not found in samples of groundwater, spring surface water and cisterns used for human supply.

The climate of the area is semi-arid, with higher precipitation from November to March averaging around 100 mm/month. During the dry season from April to October precipitation is around 19 mm/month (Figure 1B), turning the water balance temporarily negative (Santos et al. 2020). The average temperature is around 24°C, with a maximum of 30°C during the dry period and a minimum of 18.6°C during the rainy season. Rainfall intensities were obtained from the HidroWeb system of the National Water Agency for the stations in Boquira and Macaúbas (at 25 km from Boquira) from 2016 to 2019. The data were analyzed using the double mass method to confirm consistency (Santos, Anjos & Klammler 2020).

Hourly measurements of wind direction and speed data were obtained from the INMET database for Macaúbas station and the period from 2016 to 2019. Simple arithmetic (i.e., time weighted) averaging yielded estimates of monthly and annual averages. The average annual wind speed was 2.27 m/s, with a standard deviation of 0.2 m/s. The highest monthly average values observed in the dry and wet seasons were 2.57 and 1.98 m/s, respectively (Figure 1B). The topographic influence is evidenced in the pattern of wind circulation in the region that occurs predominantly in the NW-SE direction, especially in the dry period (Santos

et al. 2020). Wind behavior suggests that contaminants accumulated in the tailings basin may be transported to the urban area of Boquira (Figure 1C).

Field observations of lead concentrations were obtained in 2014 from the geochemical survey carried out by the Mineral Research and Resources Company (Cunha et al. 2016) including 59 samples of sediments from paved and unpaved streets and 110 dust samples from houses in the urban area of the municipality. The indoor dust samples were collected at locations of largest accumulation, such as roof beams, wall and furniture tops, and behind paintings. Chemical analysis consisted in ICP-OES (inductively coupled plasma atomic emission spectrometry) and ICP-MS (inductively coupled plasma mass spectrometry) on particulates < 0.18 mm (sieve size 80) using Aqua regia. The analytical results for street sediments (Figure 1C) and house dust (Figure 1D) indicated high concentrations of lead in the urban area of the municipality. Especially in the neighborhoods closest to the tailings basin (Vila Operária, Chaves, Barreiros and Centro) values ranged above the limits established by CONAMA Resolution 420/2009.

2.2 Conceptual Model

The conceptual model (Figure 2) is a synthesis of the information obtained through the collection of pre-existing data and field visits, indicating the tailings basin as a source of contamination and the urban area of the municipality representing the receiving environment. The proximity between the tailings basin and the urban area submits the latter to continuous and elevated exposure of contamination by aerial transport. Following our hypothesis, we assume that lead particulates become suspended from the tailings basin into the atmosphere, where they are transported by the turbulent action of wind in advective and dispersive ways. During transport, the particulates may be deposited in both streets and houses. Particulates in the streets tend to be resuspended by the wind, while those deposited indoors remain inactive and accumulate.



Figure 2 Conceptual model indicating the mechanisms of (re)suspension, advection, dispersion and deposition of lead particulates between the tailings basin and the urban area.

The importance of rainfall in the dispersion of contaminants is considered in the model development by promoting the deposition of suspended particles in the air and washing of the streets. However, in the present work, the results presented do not explicitly account for rainfall, but use an effective (dry plus wet) deposition mechanism instead. This assumption appears reasonable in a first approximation, because of (1) the climatic conditions in the regions with long periods of drought and low rainfall, and (2) the lack of seasonal lead concentration data for validation (only a single set of field data is available from an unknown season of the year).

2.3 Mathematical Formulation

The Eulerian approach assesses the behavior of species by describing them in relation to a fixed coordinate system, where the concentration of species in a control volume must satisfy a mass balance at every instant (Leelosy et al. 2018; Seinfeld & Pandis 2006). Here, we adopt a two-dimensional Eulerian framework, where concentrations of lead in air, streets and houses are used in dimensions of mass per unit surface area of a horizontal modeling domain (e.g., $\mu\text{g}/\text{m}^2$). This is straight-forward for streets and houses, while for air such concentrations represent the integrated mass of lead inside a vertical air column per unit horizontal surface area. Contaminant mass per unit surface area has been applied in previous studies (e.g., Andreão et al. 2020; Layton & Beamer 2009) and appears to be an appropriate measure for exposure risk and/or intensity of atmospherically transported particulates in streets and houses. For particulates suspended in the air it is a simplification to avoid the complexities of a full three-dimensional modeling effort with elevated computational cost and parameterization/data needs. Due to the same reasons and similar to previous studies (Ilyin et al. 2007; Niisoe et al. 2010), we also neglect effects of variable particulate sizes and densities to work with effective transport parameters.

For the vertically integrated lead concentration C_{ar} in an air column above ground we stipulate

$$\frac{\partial C_{air}}{\partial t} = -v_x \frac{\partial C_{air}}{\partial x} - v_y \frac{\partial C_{air}}{\partial y} + \alpha v \left(\frac{\partial^2 C_{air}}{\partial x^2} + \frac{\partial^2 C_{air}}{\partial y^2} \right) - D - L_{air} + EA_{basin} + RA_{street} \quad (1)$$

where v_x e v_y represent the horizontal components of wind speed in the directions x and y , $v = \sqrt{v_x^2 + v_y^2}$ is the absolute magnitude of wind speed, α represents the

horizontal dispersivity (here isotropic) in the atmosphere, D is the deposition term in the dry period, L_{air} is the term of air washing during rain events, E is the emission term of the contaminant from the tailings basin to the atmosphere, R is the resuspension term of the contaminant from the streets to the atmosphere, A_{basin} corresponds to the proportion of the area at each location (or in each cell of the numerical modeling mesh) occupied by the basin, and A_{street} is the proportion of the area occupied by streets. The remaining proportion is occupied by houses, i.e., $A_{house} = 1 - A_{street} - A_{basin}$. Equation 1 is a two-dimensional form of the advection-dispersion equation, where the first two terms on the right-hand-side represent advective transport, the third term in parentheses dispersive transport, and the remaining four terms represent lead mass exchange of the air with the basin, streets and houses.

From the mass balance equations for lead in the streets and houses we find

$$\frac{\partial C_{street}}{\partial t} = D - R - L_{street} \quad (2)$$

$$\frac{\partial C_{house}}{\partial t} = D \quad (3)$$

where C_{street} and C_{house} correspond to the concentrations in streets and homes, respectively; L_{street} is the term of washing the streets during rainfall.

In agreement with previous studies (Niisoe et al. 2010; Thouron et al. 2018), Equation 2 implies that the concentration on street surfaces grows with contaminant deposition from the atmosphere and decreases due to resuspension and washing of the streets during the rainy season. In contrast, the concentration in the houses is associated with deposition only without the possibility of resuspension or washing, thus leading to the effect of accumulation. Transportation by advection and dispersion in the streets and houses is considered negligible in relation to wind transport. Summation of Equation 2 after multiplication by A_{street} and Equation 3 after multiplication by A_{house} shows consistency with the mass balance of Equations 1, since contaminant mass leaving the atmosphere is exactly deposited either in the streets or in the houses, since $A_{house} + A_{street} = 1$ outside the basin (analogous for resuspension).

Due to the complexity of the particulate transport mechanisms, it is not usual to try to describe them in their most fundamental level of detail. The process of dry deposition, for example, may be represented in terms of a coefficient of deposition, which relates the flow of a species to the soil with its concentration above the surface (Evrard et al. 2015). In this way, the dry deposition flow D is

considered here as directly proportional to the atmospheric concentration C_{air} leading to

$$D = \lambda_{dep} C_{air} \tag{4}$$

where λ_{dep} is the deposition coefficient.

Dry deposition is a continuous process, while wet deposition can only occur in the presence of precipitation, when atmospheric hydrometeors collide with airborne particles collecting them as they fall (Leadbetter et al. 2020; Leelosy et al. 2018). Moreover, as the particles are removed from the air, street washing also occurs, resulting in

$$L_{air} = \lambda_{lav} P C_{air} \tag{5}$$

$$L_{street} = \lambda_{lav} P C_{street} \tag{6}$$

where P is precipitation and λ_{dep} the washing coefficient.

There is considerable uncertainty in establishing the resuspension term, due to changes in rates over time and the difficulty in quantifying traffic-induced dust resuspension on the roads. However, previous studies (Amato et al. 2012; Pant & Harrison 2013) suggest that this term can be quantified through the resuspension flux R given by

$$R = v \lambda_{res} C_{street} \tag{7}$$

where λ_{res} corresponds to the resuspension coefficient and the resuspension rate varies proportionally with the absolute magnitude v of the wind speed and the amount of contaminant available C_{street} .

Similarly, the emission flux E of the contaminant from the tailings basin into the atmosphere is represented by

$$E = v \lambda_{sus} C_{basin} \tag{8}$$

where C_{basin} corresponds to the concentration of contaminant in the basin and λ_{sus} is the suspension coefficient. Based on the large volume of tailings in the basin we assume an infinite source of contamination, i.e., $C_{basin} = constant$ (no source depletion).

2.4 Numerical Implementation

The dispersion model of Equations 1 through 3 is a set of three partial differential equations for the state variables C_{air} , C_{street} and C_{house} that are coupled by the mass fluxes for deposition D and resuspension R defined in Equations 2 and 7. An explicit finite difference solution was implemented in MATLAB R2014a, based on a horizontal Cartesian grid covering approximately 10 km² and with the lateral contours defined as zero concentration boundaries.

The grid spacing was 100 x 100 m resulting in 34 rows and 27 columns (totaling 918 cells).

The UTM coordinates (Datum SIRGAS 2000) used to define the grid were extracted from the Digital Elevation Model – MDE and the values of A_{basin} and A_{street} for each grid cell were obtained from satellite images provided by the Urban Development Company of the State of Bahia (CONDER), both using QGis 2.18.15. Thus, the modeling domain is heterogeneous in that these parameters vary in space, where it is understood that areas not occupied by the basin or streets (including open land) are houses. The spatial extent of the tailings basin was assumed to be constant as shown in Figures 1C and 1D.

The model was forced by wind velocities and directions to produce simulations of lead particulate concentrations as a function of space and time within the urban area for initial conditions of $C_{air} = C_{street} = C_{house} = 0$ everywhere. The imposed wind properties were spatially uniform, but temporally variable with an annual periodicity according to Figure 1B. Thus, after an initial warm-up period to eliminate effects of the initial conditions, simulations were limited to one-year periods with periodic extrapolation to a total exposure time of 50 years. For C_{air} and C_{street} this implies periodic repetition, while for C_{air} this means multiplication by 50 due to accumulation.

To predict the effects of complete remediation of the basin by covering its surface as a possible future scenario, for example, the simulations were simply continued with the values of C_{air} and C_{street} from above (i.e., after warm-up plus one year), but with the exception of setting $C_{basin} = 0$ and reinitializing $C_{house} = 0$. This allowed determining both the additional increase of accumulation in the houses after basin coverage as well as the reduction of C_{air} and C_{street} towards their natural background value of zero.

2.5 Calibration Procedure

The only data available for lead concentrations in the study area are in ppm of basin/street sediments and indoor dust (i.e., parts per million such as µg/g, for example). As a consequence, the actual amount of lead at a location as a natural measure for exposure risk or intensity depends on the amount of sediment or dust at that location. Unfortunately, data on spatial sediment and dust distributions are not available and their modeling is beyond the scope of this study. Instead, for the sake of demonstrating the calibration procedure and performance of our model, we assume known values of C_{basin}^{sed} , C_{street}^{sed} and C_{house}^{sed} in g/m² to represent the spatial distributions of basin/street sediment and house dust. Multiplication of these concentrations by the measurements of C_{basin}^{ppm} , C_{street}^{ppm} and C_{house}^{ppm} in ppm (as shown in Figures

1C and 1D) then yield “measured” lead concentrations in $\mu\text{g}/\text{m}^2$ consistent with the present framework.

The proposed calibration procedure of the model parameters consists of two stages: (1) preliminarily in order of magnitude using only concentrations observed immediately downstream of the tailings basin, and (2) refined with comparison of observed and simulated concentrations per model cell. The equations for the first stage are presented in general terms including C_{basin}^{sed} , C_{street}^{sed} and C_{house}^{sed} as spatially variable parameters. At the present moment however, where such detailed information is not available, we assume $C_{basin}^{sed} = C_{street}^{sed} = C_{house}^{sed} = 1 \text{ g}/\text{m}^2$ as a plausible value to allow a numerical demonstration of the calibration procedure and model performance. Note that changing this value by some factor will simply affect simulated concentrations by the same factor (equivalent to a change in concentration units). However, future studies are necessary to justify or, most likely, adjust this choice, especially considering the fact that C_{basin}^{sed} , C_{street}^{sed} and C_{house}^{sed} may be expected to be different and vary with location (see also recommendations in Section 4).

As part of the first calibration step, the observed concentrations indicated that at the exit of the tailings basin, in relation to the average direction of the winds, the highest concentrations in the houses were around $C_{house}^{ppm} \approx 10^3 \text{ ppm}$ (Figure 1D). Thus, in the period $\Delta t \approx 50$ years of existence of the tailing’s basin, Equation 3 leads to

$$D \approx \frac{C_{house}^{ppm} C_{house}^{sed}}{\Delta t} \approx 20 \frac{\mu\text{g}}{\text{m}^2 \text{yr}} \quad (9)$$

In the vicinity of the basin, where the highest values of lead concentrations were detected, and considering approximately stationary conditions ($\frac{\partial C_{street}}{\partial t} = 0$) without rain wash ($L_{street} = 0$), Equation 2 reduces to

$$D = R = v \lambda_{res} C_{street}^{ppm} C_{street}^{sed} \quad (10)$$

where last expression was obtained from Equation 7. By reformulating Equation 10 it is possible to obtain an estimate of the resuspension coefficient as

$$\lambda_{res} \approx \frac{D}{v C_{street}^{ppm} C_{street}^{sed}} \approx 10 \frac{1}{\text{yr} \frac{\text{m}}{\text{s}}} \quad (11)$$

considering an average wind speed $v \approx 2 \text{ m}/\text{s}$ (Figure 1B) and $C_{street}^{ppm} \approx 1 \text{ ppm}$ (Figure 1C).

Similarly, and also neglecting spatial gradients in the immediate vicinity downstream of the basin, Equation 1 reduces to

$$D = E = v \lambda_{sus} C_{basin}^{ppm} C_{basin}^{sed} \quad (12)$$

where the last expression was obtained from Equation 8. Knowing that within the basin the observed lead concentrations are approximately $C_{basin}^{ppm} \approx 10^4 \text{ ppm}$ (Cunha et al. 2016), it is possible to estimate the suspension coefficient as

$$\lambda_{sus} \approx \frac{D}{v C_{basin}^{ppm} C_{basin}^{sed}} \approx 10^{-3} \frac{1}{\text{yr} \frac{\text{m}}{\text{s}}} \quad (13)$$

This is much smaller than λ_{res} and may be attributed to the likely abundant presence of large lead particulates inside the tailings basin, which raise C_{basin}^{ppm} , but are not easily mobilized by the wind.

The determination of the dry deposition coefficient λ_{dep} would be possible through Equation 4, if a value for concentration C_{ar} near the basin was available. However, in the absence of an observed value, we assume that the atmospheric deposition of lead particles occurs on a time scale of a few minutes (i.e., 10^2 seconds, similar to a dust cloud behind a driving car, for example), leading to the estimation (as reciprocal value of the time scale) of

$$\lambda_{dep} \approx 10^{-2} \frac{1}{\text{s}} \quad (14)$$

For the second calibration step, simulations were conducted using a value of dispersivity $\alpha = 100 \text{ m}$ as recommended by previous studies (Kadowaki et al. 2017). Based on the first estimates from Equations 11, 13 and 14, visual adjustment of simulated against measured concentrations in Figure 3 yielded the final parameter values $\lambda_{res} = 8.84 \frac{1}{\text{yr} \frac{\text{m}}{\text{s}}}$, $\lambda_{sus} = 2.6 \times 10^{-3} \frac{1}{\text{yr} \frac{\text{m}}{\text{s}}}$ and $\lambda_{dep} = 1.2 \times 10^{-2} \frac{1}{\text{s}}$. The data points inside the red ellipse were excluded from this process, because the strong overestimation may potentially be attributed to areas of more recent construction activity and, consequently, less time for lead accumulation (50 years of exposure assumed here). The resulting root means square error in decadal concentration logarithms was 0.64, which is acceptable for concentrations ranging over almost five orders of magnitude. This is further reflected by the relative proximity of the data points with respect to the dashed line of identity in Figure 3.

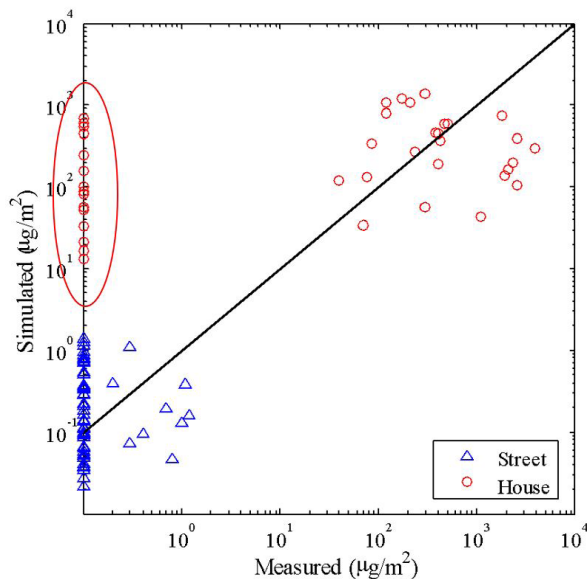


Figure 3 Model calibration of simulated (from Equations 1 through 8) versus measured lead particulate concentrations (from Figures 1C and 1D after conversion from ppm to $\mu\text{g}/\text{m}^3$) in streets and houses. The detection limit of the measurements was 0.1 ppm, i.e., $0.1 \mu\text{g}/\text{m}^3$ after conversion, and multiple measurements in a single model grid cell were averaged. The red ellipse indicates data points of C_{house} , where the model significantly overestimates observations, potentially due to more recent construction and less time of accumulation than assumed here. The black dashed line indicates identity between measured and simulated values, which differ by root means square errors in decadal concentration logarithms of 1.36 for all data and 0.64, when excluding the red ellipse (mean absolute error 0.53; correlation coefficient 0.93; mean bias 0.02).

3 Results and Discussion

The simulations performed aimed to demonstrate the atmospheric dispersion model and its calibration procedure for estimating the concentrations of lead in the air, houses and streets within the municipality of Boquira. In addition, we demonstrate the model's applicability for simulating a future scenario of a completely covered (surface sealed) tailings basin, which eliminates any further particulate suspension from the source into the atmosphere.

The simulated lead concentrations in the model cells, where field data is available (Figures 1C and 1D) are represented in Figure 4A showing an initial transience due to model warm-up of approximately 100 days. After this period, the influence of the initial conditions (all concentrations zero outside the basin) vanishes and the simulated concentrations in the air and streets reach a quasi (periodic) steady-state with a repetition of the same variability on an annual basis. This is due to the periodic

wind regime adopted in Figure 1B as a driver for lead transport. In contrast, the concentration pattern in the houses presents a relatively constant accumulation.

The simulated concentrations for model calibration (Figure 3) and spatial representation (Figure 5A) were obtained as the values at $t = 400$ d in Figure 4A. Near the basin, simulated values of C_{street} varied from 1 to $1.5 \mu\text{g}/\text{m}^3$. For the accumulated concentrations C_{house} inside the houses, we multiplied the respective accumulation during the final 365 days of the simulation by the exposure time of the basin (50 years), obtaining concentrations ranging from 1000 to $1500 \mu\text{g}/\text{m}^3$ near the basin (Figure 5A). Using Equation 4 and inspection of Figure 4A further show that $C_{\text{air}} \approx 10^{-4} \mu\text{g}/\text{m}^3$, i.e. significantly below C_{street} , which is on the order of 10^0 , and C_{house} on the order of 10^3 . As to be expected, this reflects that most of the lead is concentrated in the houses, followed by streets and suspended in the air. This is consistent with previous studies (Fung, Yang & Zhu 2014; Leung 2015) showing higher contaminant concentrations in internal areas with respect to outdoor.

The calibration graph indicates that the largest errors are associated with measurements of C_{house} at the detection limit of $0.1 \mu\text{g}/\text{m}^3$ (Figure 3, red ellipse). We hypothesize that this strong overestimation is due to the shorter time available for accumulation of this contaminant in more recently constructed parts of the urban area. This is supported by the fact that these data points are indeed located in the Urban Expansion Zone with the most recent constructions established in the Participatory Master Plan of the municipality, especially in the Barreiros neighborhood.

The origin and process of urban expansion of the municipality are related to the discovery and extraction of lead in the 1950s, when starting the construction of the Vila Operária to house the workers of the mining company immediately next to the tailings basin. For both houses and streets, the most distant points below the line of identity in Figure 3 are located in Vila Operária, which is somewhat off the average direction of the wind from the basin, hence resulting in a tendency of the model to underestimate observed concentrations.

Considering the hypothetical remediation scenario of a complete sealing of the tailings basin's surface to discontinue the release of lead into the atmosphere, it can be observed that C_{air} and C_{street} decrease considerably towards zero after 200 days (Figure 4B). During the same time, C_{house} still suffers an increase of approximately $1 - 3 \mu\text{g}/\text{m}^3$ in the most affected locations and then stabilizes, which reflects the absence of any further lead in the outdoor area, as observed in the graphs of C_{air} and C_{street} . This is in agreement with Layton and Beamer (2009), who concluded that after source elimination, resuspension from the soil becomes the principal lead source for houses.

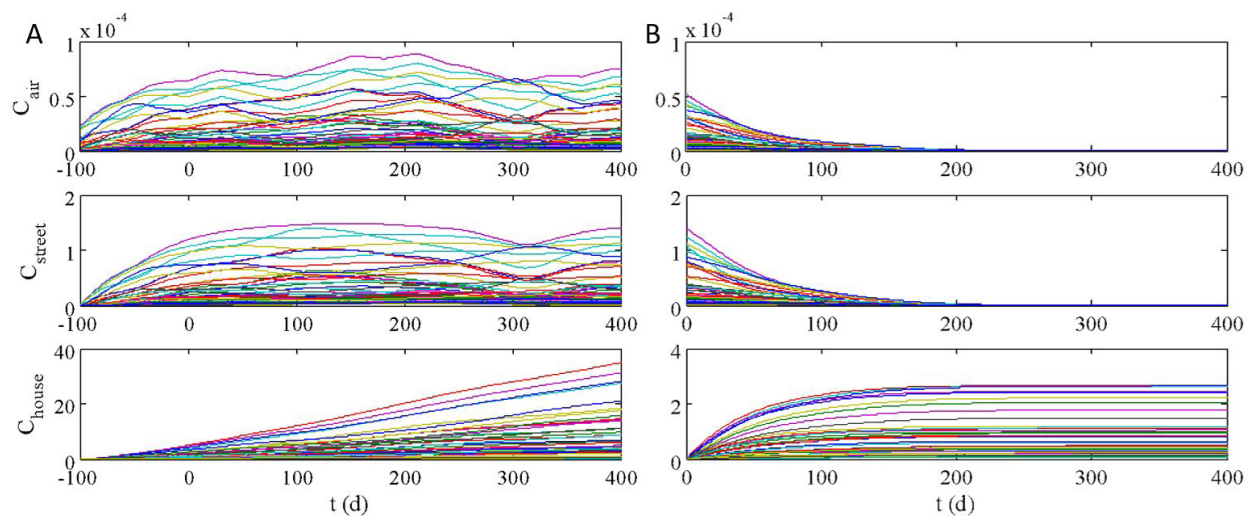


Figure 4 Time series of simulated lead particulate concentrations in $\mu\text{g}/\text{m}^2$ at the model grid cells, where field data is available (see Figures 1C and 1D). A. Warm-up period ($t < 0$) and approximately one year of simulation with the active basin; B. Approximately one year of simulation after hypothetical basin cover.

The temporal evolution of the spatial lead distribution for this scenario is illustrated in Figures 5B, 5C and 5D for 100, 200 and 400 days after coverage. The plumes in the air and streets are seen to move away from the basin in the direction of the wind, while losing intensity (note the decreasing ranges of the color scales with time). In contrast, the plume of accumulated lead inside the houses remains stationary and concentrations slightly grow to a stable level (compare discussion with Figure 4B).

An interesting aspect that is most obvious in Figure 5D is the apparent division of the plume into three disconnected parts. This may be explained by the highest densities of urbanization in the zones between the plume parts, where the large presence of houses acts as a strong sink for lead particulates, thus strongly reducing C_{air} and C_{street} in those locations. Also of interest is the extremely slow movement of the suspended plume (C_{air} in left column of Figure 5) with respect to the average wind speed of approximately 2 m/s. This may be attributed to the retarding effect of deposition and resuspension. In other words, a particulate only travels at the speed of wind for a short time before it is deposited on the ground to remain stationary for a significantly longer period awaiting subsequent mobilization by resuspension. This effect becomes stronger at smaller wind velocities, where resuspension is weaker and, hence, a larger portion of particulates remains in immobile deposition (Quan et al. 2020; Zhang et al. 2021).

The present model is based on several conceptual and mathematical simplifications to facilitate tractability and to meet a reasonable level of consistency with the limited

amount of information available for parameterization. Most fundamentally, we assume that atmospheric particulate transport can be described by the two-dimensional advection-dispersion equation and that mass transfer between air and the basin, streets and houses can be represented by effective transport parameters. This, for example, neglects the influence of variable particulate sizes and densities on transport properties, and the vertical particulate distribution in the atmosphere.

Although included in the model equations, the washing effect of rainfall, especially on the streets, is not explicitly accounted for in this first model demonstration. Additional information on the timing of field sample collection with respect to rainfall events (or even seasons) would be required to assure the possibility of a reasonable parameterization of this mechanism. Finally, and very fundamentally, this study is limited by the available field data on lead concentrations reported in ppm, i.e., mass of lead per mass of street sediment or house dust. This is clearly not a sufficient metric to quantify lead exposure, which would still require additional knowledge about the amounts of sediment or dust at a location. Instead, we formulate our lead dispersion/exposure model in units of mass per surface area and assume a constant amount of sediment/house dust per area to convert field measurements from ppm to $\mu\text{g}/\text{m}^2$. This is a strong assumption requiring future studies for validation and adjustment, but it appears appropriate for the sake of demonstrating the model and calibration procedure developed here.

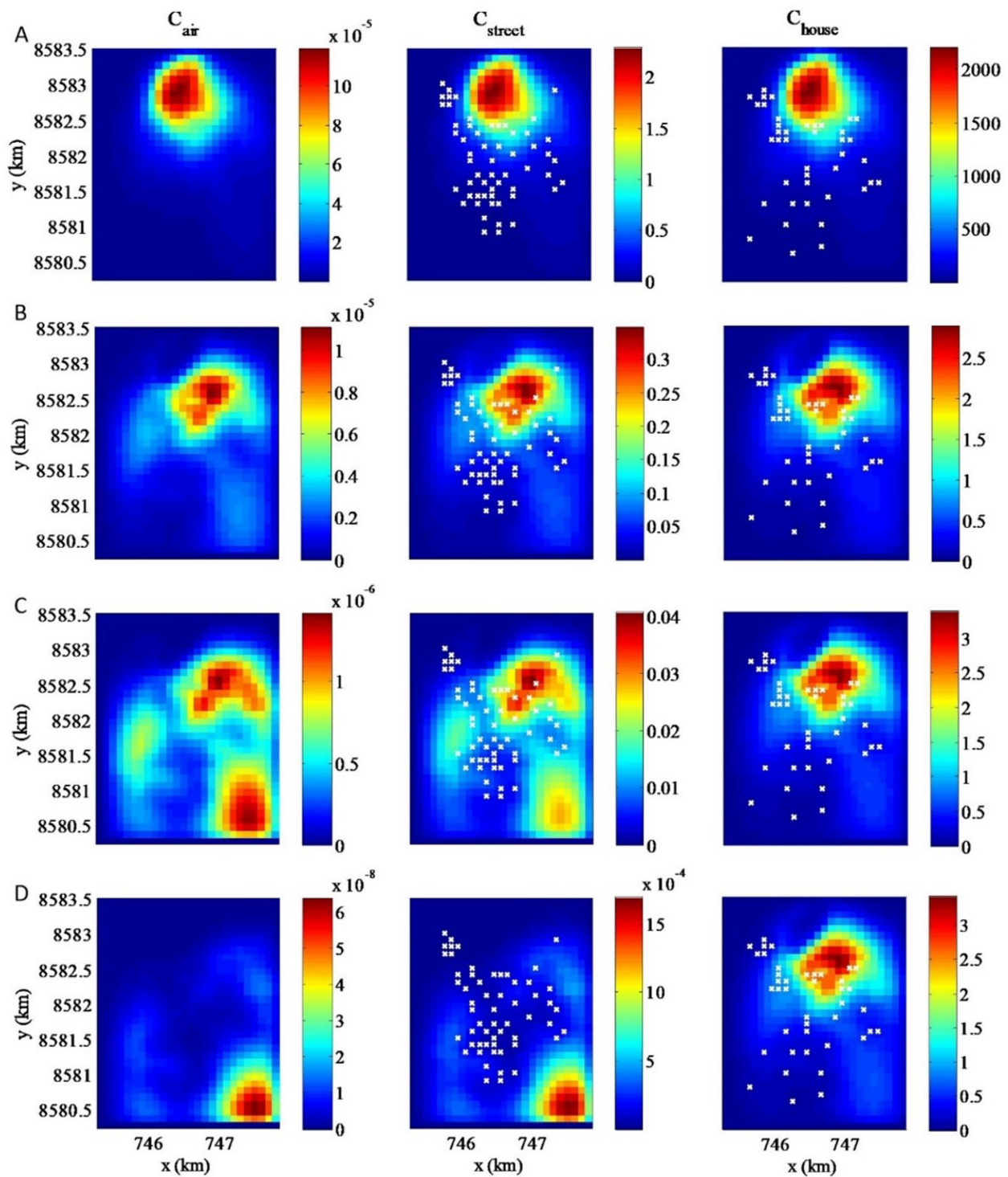


Figure 5 Spatial distributions of lead concentrations in $\mu\text{g}/\text{m}^3$ in the air (left column), streets (center column) and houses (right column) with grid cells where field data are available (white crosses; compare Figures 1C and 1D). Row A. At the end of 400 days of simulation with the active basin (see Figure 4A); Rows B, C and D. At 100, 200 and 400 days after basin coverage, respectively (see Figure 4B).

4 Conclusion

Modeling results satisfactorily reproduce the orders of magnitude of measured lead concentrations in streets and houses, thus supporting the hypotheses of resuspension from streets as opposed to accumulation in houses. Application of the model to a hypothetical future scenario of source removal (e.g., basin coverage) shows that lead concentrations in the air and streets are significantly reduced after approximately 200 days, while accumulated concentrations indoors reach a constant level and require other measures for remediation (e.g., removal by cleaning). Modeling results of this kind may have potential to support public management in the establishment of policies that contribute to the improvement of the municipality's environmental quality.

Direct implications of this study include the recommendation to perform future field sampling campaigns for quantifying exposure risk with the goal of measuring contaminant concentrations in mass per surface area instead of ppm. This appears relatively straight-forward for open areas, but will require some future refinements for indoor sampling, where parts of a house may be regularly cleaned versus others that are not. Additional sampling of lead concentrations in the air as the only responsible transport medium would also be highly valuable. Such a sampling could be flux-based using filters or traps that remain stationary and in operation over a certain period of time.

Further implications include the necessity to perform additional or even regularly repeated field sampling campaigns. Only such data could ultimately confirm the hypothesis of lead accumulation in houses and, if done frequently enough, provide sufficient information to evaluate/parameterize the effects of rainfall washing. For this purpose, we recommend the installation of a number of fixed air filters and sediment/dust traps for regular (e.g., monthly to capture seasonal effects) sampling under controlled conditions throughout the urban area.

5 Acknowledgments

We are grateful to Drs. Sandro L. Machado, Francisco I. Negrão, Maria C.R. Gomes, Ricardo G.F.A. Pereira and two anonymous reviewers for their constructive comments, which contributed significantly to improve the revised version of the manuscript.

6 References

Alkmim, F.F., Brito Neves, B.B. & Alves, I.A.C. 1993, 'Arcabouço Tectônico do Cráton do São Francisco - uma revisão', in J.M.L.

- Dominguez & A. Misi (eds), *O Cráton do São Francisco: Trabalhos apresentados na reunião preparatória do II Simpósio sobre o Cráton do São Francisco*, SBG, Salvador, pp. 45-62.
- Amato, F., Karanasiou, A., Moreno, T., Alastuey, A., Orza, J.A.G., Lumbreras, J., Borge, R., Boldo, E., Linares, C. & Querol, X. 2012, 'Emission factors from road dust resuspension in a Mediterranean freeway', *Atmospheric Environment*, vol. 61, pp. 580-7, DOI:10.1016/j.atmosenv.2012.07.065.
- Andreão, W.L., Pinto, J.A., Pedruzzi, R., Kumar, P. & Albuquerque, T.T.A. 2020, 'Quantifying the impact of particulate matter on mortality and hospitalizations in four Brazilian metropolitan areas', *Journal of Environmental Management*, vol. 270, 110840, DOI:10.1016/j.jenvman.2020.110840.
- Borges, R.R., Teixeira, A.C.R. & Ribeiro, F.N.D. 2021, 'Modelagem da dispersão atmosférica de material particulado (MP10) e os impactos da utilização de veículos de carga movidos a GNL em São Paulo', *Revista do Departamento de Geografia*, vol. 41, no. 1, e185828, DOI:10.11606/eISSN.2236-2878.rdg.2021.185828.
- Carvalho, I.G., Iyer, S.S.S., Tassinari, C.C.G. & Misi, A. 1997, 'Lead and sulfur-isotope investigations of the Boquira sediment-hosted sulfide deposits, Brazil', *International Geology Review*, vol. 39, no. 2, pp. 97-106, DOI:10.1080/00206819709465261.
- Chen, H., Wang, L., Hu, B., Xu, J. & Liu, X. 2022, 'Potential driving forces and probabilistic health risks of heavy metal accumulation in the soils from an e-waste area, southeast China', *Chemosphere*, vol. 289, 133182, DOI:10.1016/j.chemosphere.2021.133182.
- Christou, A., Hadjisterkotis, E., Dalias, P., Demetriou, E., Christofidou, M., Kozakou, S., Michael, N., Charalambous, C., Hatzigeorgiou, M., Christou, E., Stefani, D., Christoforou, E. & Neocleous, D. 2022, 'Lead contamination of soils, sediments, and vegetation in a shooting range and adjacent terrestrial and aquatic ecosystems: A holistic approach for evaluating potential risks', *Chemosphere*, vol. 292, 133424, DOI:10.1016/j.chemosphere.2021.133424.
- Costa, E.S. & Costa, A.A. 2021, 'Study of the transport of atmospheric pollutants in the Pecém Industrial and Port Complex (CIPP), Ceará, Brazil', *Revista Brasileira de Meteorologia*, vol. 36, no. 3, pp. 615-24, DOI:10.1590/0102-77863630030.
- Cunha, F.G., Viglio, E.P., Anjos, J.A.S.A. & Loureiro, T.B. 2016, *Estudos geoquímicos no município de Boquira - Estado da Bahia*, CPRM, Salvador.
- Duarte, E.S.F., Franke, P., Lange, A.C., Friese, E., Lopes, F.J.S., Silva, J.J., Reis, J.S., Landulfo, E., Silva, C.M.S., Elbern, H. & Hoelzemann, J.J. 2021, 'Evaluation of atmospheric aerosols in the metropolitan area of São Paulo simulated by the regional EURAD-IM model on high-resolution', *Atmospheric Pollution Research*, vol. 12, no. 2, pp. 451-69, DOI:10.1016/j.apr.2020.12.006.
- Evrard, O., Lacey, J.P., Lepage, H., Onda, Y., Cerdan, O. & Ayrault, S. 2015, 'Radiocesium transfer from hillslopes to the Pacific Ocean after the Fukushima nuclear power plant

- accident: A review', *Journal of Environmental Radioactivity*, vol. 148, pp. 92-110, DOI:10.1016/j.jenvrad.2015.06.018.
- Fung, C.C., Yang, P. & Zhu, Y.F. 2014, *Infiltration of diesel exhaust into a mechanically ventilated building*, Paper#HP0626, Indoor Air, Hong Kong.
- Garcia, P.M.P. 2011, 'Análise comparativa de dados geológicos, litogeoquímicos e geofísicos das formações ferríferas do Complexo Boquira e supergrupo espinhaço na região de Boquira, BA', Bachelor thesis, Universidade Federal da Bahia, Salvador.
- Giovannini, L., Ferrero, E., Karl, T., Rotach, M.W., Staquet, C., Castelli, S.T. & Zardi, D. 2020, 'Atmospheric pollutant dispersion over complex terrain: Challenges and needs for improving air quality measurements and modeling', *Atmosphere*, vol. 11, no. 6, pp. 646-78, DOI:10.3390/atmos11060646.
- Gomes, M.C.R., Anjos, J.A.S.A. & Daltro, R.R. 2020, 'Multivariate statistical analysis applied to the evaluation of groundwater quality in the central-southern portion of the state of Bahia - Brazil', *Revista Ambiente & Água*, vol. 15, no. 1, e2408, DOI:10.4136/ambi-agua.2408.
- Huang, Y., Dang, F., Li, M., Zhou, D., Song, Y. & Wang, J. 2020, 'Environmental and human health risks from metal exposures nearby a Pb-Zn-Ag mine, China', *Science of The Total Environment*, vol. 698, 134326, DOI:10.1016/j.scitotenv.2019.134326.
- Ilyin, I., Rozovskaya, O., Sokovykh, V. & Travnikov, O. 2007, *Atmospheric modelling of heavy metal pollution in Europe: Further development and evaluation of the MSCE-HM model*, Meteorological Synthesizing Centre e East of EMEP, Moscow.
- Kadowaki, M., Katata, G., Terada, H. & Nagai, H. 2017, 'Desenvolvimento do modelo Euleriano de transporte atmosférico GEARN-FDM: Validação contra o experimento europeu do traçador', *Atmospheric Pollution Research*, vol. 8, no. 2, pp. 394-402.
- Khan, S. & Hassan, Q. 2021, 'Review of developments in air quality modelling and air quality dispersion models', *Journal of Environmental Engineering and Science*, vol. 16, no. 1, pp. 1-10, DOI:10.1680/jenes.20.00004.
- Layton, D. & Beamer, P. 2009, 'Migration of contaminated soil and airborne particulates to indoor dust', *Environmental Science & Technology*, vol. 43, no. 21, pp. 8199-205, DOI:10.1021/es9003735.
- Leadbetter, S.J., Andronopoulos, S., Bedwell, P., Chevalier-Jabet, K., Geertsema, G., Gering, F., Hamburger, T., Jones, A.R., Klein, H., Korsakissok, I., Mathieu, A., Pázmándi, T., Périllat, R., Rudas, C., Sogachev, A., Szántó, P., Tomas, J.M., Twenhöfel, C., Vries, H. & Wellings, J. 2020, 'Ranking uncertainties in atmospheric dispersion modelling following the accidental release of radioactive material', *Radioprotection*, vol. 55, no. 1, pp. 51-5, DOI:10.1051/radiopro/2020012.
- Leelossy, A., Lagzi, I., Kovács, A. & Mészáros, R. 2018, 'A review of numerical models to predict the atmospheric dispersion of radionuclides', *Journal of Environmental Radioactivity*, vol. 182, pp. 20-33, DOI:10.1016/j.jenvrad.2017.11.009.
- Leung, D.Y.C. 2015, 'Outdoor-indoor air pollution in urban environment: challenges and opportunity', *Frontiers in Environmental Science*, vol. 2, pp. 280-95, DOI:10.3389/fenvs.2014.00069.
- Niisoe, T., Nakamura, E., Harada, K., Ishikawa, H., Hitomi, T., Watanabe, T., Wang, Z. & Koizumi, A. 2010, 'A global transport model of lead in the atmosphere', *Atmospheric Environmental*, vol. 44, no. 14, pp. 1806-14, DOI:10.1016/j.atmosenv.2010.01.001.
- Pant, P. & Harrison, R.M. 2013, 'Estimation of the contribution of road traffic emissions to particulate matter concentrations from field measurements: A review', *Atmospheric Environment*, vol. 77, pp. 78-97, DOI:10.1016/j.atmosenv.2013.04.028.
- Quan, J., Dou, Y., Zhao, X., Liu, Q., Sun, Z., Pan, Y., Jia, X., Cheng, Z., Ma, P., Su, J., Xin, J. & Liu, Y. 2020, 'Regional atmospheric pollutant transport mechanisms over the North China Plain driven by topography and planetary boundary layer processes', *Atmospheric Environmental*, vol. 221, 117098, DOI:10.1016/j.atmosenv.2019.117098.
- Santos, N.L., Anjos, J.A.S.A. & Klammler, H. 2020, 'Exposição da Zona Urbana de Boquira, estado da Bahia, aos Metais Tóxicos Associados à Bacia de Rejeito de Mineração Abandonada', *Anuário do Instituto de Geociências*, vol. 43, no. 3, pp. 280-91, DOI:10.11137/2020_3_280_291.
- Seinfeld, J.H. & Pandis, S.N. 2006, *Atmospheric chemistry and physics: From air pollution to climate change*, 2nd edn, John Wiley & Sons, New York.
- Teixeira, D.C.L., Moreira, F.V., Coelho, M.A., Amaral, F.Q. & Cupertino, M.C. 2020, 'Exposição a contaminantes ambientais inorgânicos e danos à saúde humana', *Brazilian Journal of Health Review*, vol. 3, no. 4, pp. 10353-69, DOI:10.34119/bjhrv3n4-256.
- Thouron, L., Seigneura, C., Kim, Y., Mahé, F., André, M., Lejri, D., Villegas, D., Bruge, B., Chanut, H. & Pellan, Y. 2018, 'Intercomparison of three modeling approaches for traffic-related road dust resuspension using two experimental data sets', *Transportation Research Part D: Transport and Environment*, vol. 58, pp. 108-21, DOI:10.1016/j.trd.2017.11.003.
- WHO World Health Organization 2016, *World Health Organization ambient air pollution: A global assessment of exposure and burden of disease*, World Health Organization, Geneva, viewed 4 February 2022, <<https://apps.who.int/iris/handle/10665/250141>>.
- WHO World Health Organization 2017, *Recycling used lead-acid batteries: Health considerations*, World Health Organization, Geneva, viewed 4 February 2022, <<https://apps.who.int/iris/handle/10665/259447>>.
- WHO World Health Organization 2021, *Guideline for clinical management of exposure to lead*, World Health Organization, Geneva, viewed 4 February 2022, <<https://www.who.int/publications/i/item/9789240037045>>.
- Zhang, W., Hai, S., Zhao, Y., Sheng, L., Zhou, Y., Wang, W. & Li, W. 2021, 'Numerical modeling of regional transport of PM_{2.5} during a severe pollution event in the Beijing-Tianjin-Hebei region in November 2015', *Atmospheric Environment*, vol. 254, 118393, DOI:10.1016/j.atmosenv.2021.118393.

How to cite:

Santos, N.L., Klammler, H. & Leal, L.R.B. 2022, 'Modeling Urban Atmospheric Lead Dispersion from a Mining Tailings Basin in Bahia, Brazil', *Anuário do Instituto de Geociências*, 45:48909. https://doi.org/10.11137/1982-3908_45_48909

Author contributions

Nelize Lima dos Santos: conceptualization; formal analysis, methodology; validation; writing – original draft; writing review and editing; funding acquisition; supervision; visualization. **Harald Klammler:** conceptualization; formal analysis, methodology; validation; writing – original draft; writing review and editing; funding acquisition; supervision; visualization. **Luís Rogério Bastos Leal:** writing review and editing; supervision.

Conflict of interest

The authors declare no potential conflict of interest.

Data availability statement

All data included in this study are publicly available in the literature.

Funding information

Brazilian Coordination for the Improvement of Higher Education Personnel (CAPES); process 88882.452960 / 2019-01.

Editor-in-chief

Dr. Claudine Dereczynski

Associate Editor

Dr. Fernanda Cerqueira Vasconcellos